Journal of Alloys and Compounds 509 (2011) 3435–3440

Contents lists available at ScienceDirect

Journal of Alloys and Compounds

journal homepage: www.elsevier.com/locate/jallcom

Magnetic properties of the 1/1 approximant $Ag_{42}In_{42}Gd_{16}$ to the icosahedral quasicrystal Ag–In–Gd

P. Wang[a], Z.M. Stadnik[a,*], J. Przewoźnik[b]

[a] Department of Physics, University of Ottawa, Ottawa, Ontario K1N 6N5, Canada
[b] Solid State Physics Department, Faculty of Physics and Applied Computer Science, AGH University of Science and Technology, 30-059 Kraków, Poland

ARTICLE INFO

Article history:
Received 14 August 2010
Received in revised form
21 September 2010
Accepted 22 September 2010
Available online 4 December 2010

PACS:
61.44.Br
75.50.Kj
75.50.Lk
76.80.+y

Keywords:
Approximant to a quasicrystal
Spin glass
^{155}Gd Mössbauer spectroscopy

ABSTRACT

The structural, magnetic, and ^{155}Gd Mössbauer spectral properties of the 1/1 approximant $Ag_{42}In_{42}Gd_{16}$ to an icosahedral quasicrystal Ag–In–Gd are reported. Based on dc magnetic susceptibility measurements, it is shown that the studied compound develops no long-range magnetic order in the temperature range 1.8–300 K. The dc zero-field-cooled and field-cooled susceptibility data indicate that the 1/1 approximant $Ag_{42}In_{42}Gd_{16}$ is a spin glasss with freezing temperature $T_f = 3.6(1)$ K. This is further confirmed by the analysis of the frequency dependence of T_f using the Vogel–Fulcher law and the dynamic scaling behavior near T_f. It is argued that the spin freezing process is a true equilibrium phase transition rather than a nonequilibrium phenomenon. The large frustration parameter of the studied compound indicates that it belongs to a category of strongly geometrically frustrated magnets. The ^{155}Gd Mössbauer spectra of the 1/1 approximant $Ag_{42}In_{42}Gd_{16}$ confirm that the Gd spins are frozen at 1.5 K and are fluctuating at 4.6 K. The Debye temperature of the 1/1 approximant $Ag_{42}In_{42}Gd_{16}$ is 200(1) K.

1. Introduction

Quasicrystals (QCs), which were discovered more than a quarter century ago [1], are a new form of solid which differs from the other two known forms, crystalline and amorphous, by possessing a new type of long-range translational order, quasiperiodicity, and a noncrystallographic orientational order associated with classically forbidden fivefold, eightfold, tenfold, and twelvefold symmetry axes [2]. One of the central problems in solid-state physics is determining whether quasiperiodicity leads to novel physical properties which are significantly different from those of crystalline and amorphous compounds of the same/similar compositions.

Until recently, all known thermodynamically stable QCs were ternary or quaternary alloys. The first, thermodynamically stable, binary icosahedral (*i*) QCs $YbCd_{5.7}$ and $CaCd_{5.7}$ were discovered by Tsai et al. [3] This has led to the finding of several ternary *i* QCs by total or partial replacement of Yb or Ca and Cd with other metallic elements. In particular, by replacing Yb with rare-earth (RE) elements and Cd with Ag and In, a series of new Ag–In–RE *i* QCs was found [4,5]. From this seris, the physical properties of only *i* Ag–In–Yb QCs (Ref. [6]) and *i* $Ag_{50}In_{36}Gd_{14}$ QC (Ref. [7]) were investigated.

A so-called approximant to a QC is a structurally complex crystalline compound close in composition to the QC that contains the arrangement of atoms in its usually large unit cell that is similar to the local atomic structure of the QC [8,9]. Cubic crystalline compounds $YbCd_6$ and $CaCd_6$ are 1/1 approximants to the *i* QCs $YbCd_{5.7}$ and $CaCd_{5.7}$, respectively [10,11]. A similar replacement in $YbCd_6$ of Yb with RE elements and Cd with Ag and In has led to the discovery of ternary Ag–In–RE 1/1 approximants to the Ag–In–RE *i* QCs [5,12]. The availability of the *i* and 1/1 approximant Ag–In–RE compounds of the similar composition allows for a study of the influence of quasiperiodicity on the physical properties of these alloys. In this paper, we report on structural, magnetic, and ^{155}Gd Mössbauer spectroscopy studies of the 1/1 crystalline approximant $Ag_{42}In_{42}Gd_{16}$ to the *i* $Ag_{50}In_{36}Gd_{14}$ QC.

2. Experimental methods

To synthesize the 1/1 approximant $Ag_{42}In_{42}Gd_{16}$, starting elements in the form of Ag shots (purity, 99.99%), In shots (purity, 99.999%), and Gd chunks (purity, 99.9%) were used as received. Appropriate amounts of these elements corresponding to the composition $Ag_{42}In_{42}Gd_{16}$ were weighed (±0.1 mg) and weld-sealed under an argon atmosphere into a tantalum container. The container was in turn held within an evacuated SiO_2 jacket to avoid oxidation in air. The mixture was melted using an induction furnace.

* Corresponding author.
E-mail address: stadnik@uottawa.ca (Z.M. Stadnik).

0925-8388/$ – see front matter © 2010 Elsevier B.V. All rights reserved.
doi:10.1016/j.jallcom.2010.09.214

X-ray diffraction measurements were carried out at 298 K in Bragg–Brentano geometry on the PANalytical X'Pert scanning diffractometer using Cu $K\alpha$ radiation. The $K\beta$ line was eliminated by using a Kevex PSi2 Peltier-cooled solid-state Si detector. In order to avoid deviation from intensity linearity of the solid-state Si detector, its parameters and the parameters of the diffractometer were chosen in such a way as to limit the count rate from the most intense Bragg peaks to less than 9000 counts/s [13].

The dc magnetic susceptibility was measured with a Quantum Design (QD) Magnetic Property Measurement System in the temperature range 1.8–300 K. The ac magnetic susceptibility data were collected in a QD Physical Property Measurement System between 2.0 and 20 K in a 1 Oe ac magnetic field and zero external magnetic field for frequencies varying from 300 Hz to 10 kHz.

The ^{155}Gd Mössbauer measurements were done using a standard Mössbauer spectrometer operating in a sine mode and a source of ^{155}Eu(SmPd$_3$). The source was kept at the same temperature as that of the absorber. The spectrometer was calibrated with a Michelson interferometer [14], and the spectra were folded. The Mössbauer absorber was made of pulverized material pressed into a pellet which was inserted into an Al disk container of thickness of 0.008 mm to ensure a uniform temperature over the whole Mössbauer absorber. The surface density of the Mössbauer absorber of the 1/1 approximant $Ag_{42}In_{42}Gd_{16}$ was 345 mg/cm^2. The 86.5 keV γ-rays were detected with a 2.5 cm NaI(Tl) scintillation detector covered with a 0.6 mm Pb plate to cut off the 105.3 keV γ-rays emitted from the source.

The analysis of the Mössbauer spectra involved a least-squares fitting procedure which entailed calculations of the positions and relative intensities of the absorption lines by numerical diagonalization of the full hyperfine interaction Hamiltonian. In the principal axis coordinate system of the electric field gradient (EFG) tensor, the Hamiltonian can be written as [15]

$$\hat{H} = g\mu_B H_{hf}\left[\hat{I}_z\cos\theta + \frac{1}{2}(\hat{I}_+ e^{-i\phi} + \hat{I}_- e^{i\phi})\sin\theta\right] + \frac{eQV_{zz}}{4I(2I-1)}\left[3\hat{I}_z^2 - I(I+1) + \frac{\eta}{2}(\hat{I}_+^2 + \hat{I}_-^2)\right], \quad (1)$$

where g is a nuclear g-factor of a nuclear state, μ_B is the nuclear Bohr magneton, H_{hf} is the hyperfine magnetic field at a nuclear site, Q is the quadrupole moment of a nuclear state, I is the nuclear spin, V_{zz} is the z component of the EFG tensor, η is the asymmetry parameter defined as $\eta = |(V_{xx} - V_{yy})/V_{zz}|$ (if the principal axes are chosen such that $|V_{xx}| < |V_{yy}| < |V_{zz}|$, then $0 \le \eta \le 1$), θ is the angle between the direction of H_{hf} and the V_{zz}-axis, ϕ is the angle between the V_{xx}-axis and the projection of H_{hf} onto the xy plane, and the $\hat{I}_z$, $\hat{I}_+$, and $\hat{I}_-$ operators have their usual meaning. During the fitting procedure, the g factor and the quadrupole moment ratios for ^{155}Gd ($I_g = 3/2$, $I_{ex} = 5/2$) were constrained to $g_{ex}/g_g = 1.235$ and $Q_{ex}/Q_g = 0.087$, respectively [16]. The interference factor ξ for the E1 transition of 86.5-keV in ^{155}Gd was fixed to the value of 0.0520 which was derived from the fit of the ^{155}Gd Mössbauer spectrum of $GdFe_2$ at 4.2 K [17].

A transmission integral formula was used to describe the resonance line shape of the Mössbauer spectra [18]. In addition to the hyperfine parameters, only the absorber Debye–Waller factor f_a and the absorber linewidth Γ_a were fitted as independent parameters. The source linewidth $\Gamma_s = 0.334$ mm/s and the background-corrected Debye–Waller factor of the source f_s^* [18], which were derived from the fit of the ^{155}Gd Mössbauer spectrum of $GdFe_2$ at 4.2 K [17], were used. The ^{155}Eu(SmPd$_3$) source at 1.5 K emits a broadened emission line; it was found from the fit of the ^{155}Gd Mössbauer spectrum of $GdFe_2$ at 1.5 K that $\Gamma_s = 0.708$ mm/s [17].

3. Results and discussion

3.1. Structural characterization

The 1/1 approximant $Ag_{42}In_{42}Gd_{16}$ crystallizes in the $YbCd_6$-type crystal structure [11] with the space group $Im\bar{3}$ (no. 204). There are 24 formula units of $(Ag,In)_6Gd$ per unit cell. Fig. 1 shows the X-ray powder diffraction pattern of the 1/1 approximant $Ag_{42}In_{42}Gd_{16}$. In the Rietveld refinement [19], the atomic positions for the Ag, In, and Gd sites and their occupancies were fixed to the positions and occupancies, respectively, for the Cd and Gd sites in the $GdCd_6$ approximant [11]. The Rietveld refinement of the X-ray powder diffraction data was performed (Fig. 1), yielding the lattice parameter $a = 15.207(1)$ Å. The reliability factors [19] of the refinement were $R_p = 10.7\%$, $R_{wp} = 15.8\%$, and $\chi^2 = 14.1$. The sample studied contains second phases of Ag_2InGd (space group $Fm\bar{3}m$) in the amount of 14.3 wt%, $Ag_{0.5}In_{0.5}Gd$ (space group $Pm\bar{3}m$) in the amount of 3.0 wt%, as determined from the Rietveld refinement of the XRD pattern (Fig. 1), and the third second phase that could not be identified. The large values of the reliability factors result from the fact that it was not possible to include the third second phase in the refinement.

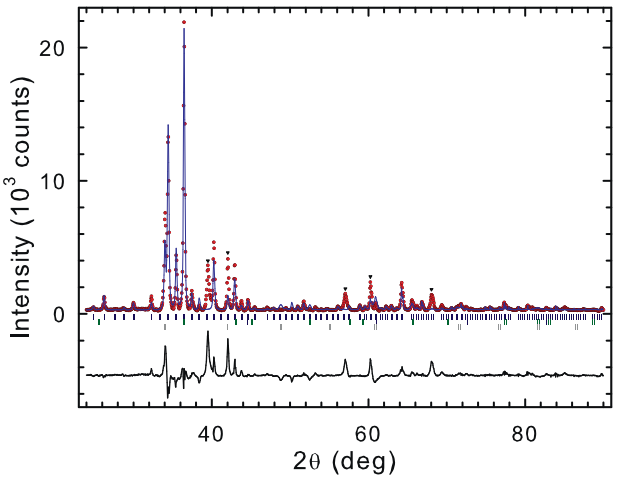

Fig. 1. The X-ray diffraction spectrum of the 1/1 approximant $Ag_{42}In_{42}Gd_{16}$ at 298 K. The experimental data are denoted by open circles, while the line through the circles represents the results of the Rietveld refinement. The upper set of vertical bars represents the Bragg peak positions corresponding to the principal $Ag_{42}In_{42}Gd_{16}$ phase, while the lower two sets refer to the positions of the impurity phases of Ag_2InGd (space group $Fm\bar{3}m$) and $Ag_{0.5}In_{0.5}Gd$ (space group $Pm\bar{3}m$). The symbol ▼ indicates the peak positions corresponding to an unidentified impurity phase. The lower solid line represents the difference curve between experimental and calculated spectra.

The lattice constant a of a 1/1 approximant to an i QC and the six-dimensional hypercubic lattice constant a_{6D} of the i QC are related through the relation $a = \sqrt{2/(2+\tau)}(1+\tau)a_{6D}$, where τ is the golden mean $\left[\tau = (1+\sqrt{5})/2\right]$ [9]. Using the value $a_{6D} = 7.805$ Å for the i QC $Ag_{50}In_{36}Gd_{14}$ [7], one would expect that $a = 15.192$ Å, which is in reasonable agreement with the value of 15.207 Å obtained from the Rietveld refinement.

3.2. Magnetic measurements

3.2.1. Dc magnetic susceptibility

The magnetic susceptibility χ of the i QC $Ag_{50}In_{36}Gd_{14}$ showed irreversibility between field-cooled (FC) and zero-field cooled (ZFC) conditions [7]. This was taken as evidence that this QC is a spin glass with the spin freezing temperature $T_f = 4.25(5)$ K [7].

Fig. 2(a) shows the temperature dependence of the magnetic susceptibility χ of the 1/1 approximant $Ag_{42}In_{42}Gd_{16}$ measured in an applied magnetic field of 50 Oe. The sample was field-cooled to 1.8 K and the measurement was carried out while warming the sample up to 300 K. The $\chi(T)$ curve has a peak at 3.4(1) K [inset in Fig. 2(a)] which indicates magnetic ordering. The $\chi(T)$ data above 20 K were fitted to a modified Curie–Weiss law

$$\chi = \chi_0 + \frac{C}{T - \Theta_p}, \quad (2)$$

where χ_0 is the temperature-independent magnetic susceptibility, C is the Curie constant, and Θ_p is the paramagnetic Curie temperature. The Curie constant can be expressed as $C = (N\mu_{eff}^2)/(3k_B)$, where N is the concentration of magnetic atoms per unit mass, μ_{eff} is the effective magnetic moment, and k_B is the Boltzmann constant. The inverse magnetic susceptibility corrected for the contribution χ_0, $(\chi - \chi_0)^{-1}$, versus temperature is shown in Fig. 2(b); the data clearly satisfy the modified Curie–Weiss law. The values of χ_0, C, and Θ_p obtained from the fit are, respectively, $1.68(18) \times 10^{-6}$ emu/g [$1.25(14) \times 10^{-3}$ emu/(mol Gd)], $10.4(1) \times 10^{-3}$ emu K/g, and $-73.6(5)$ K. This value of C corresponds to $\mu_{eff} = 7.86(23)\ \mu_B$ per Gd atom.

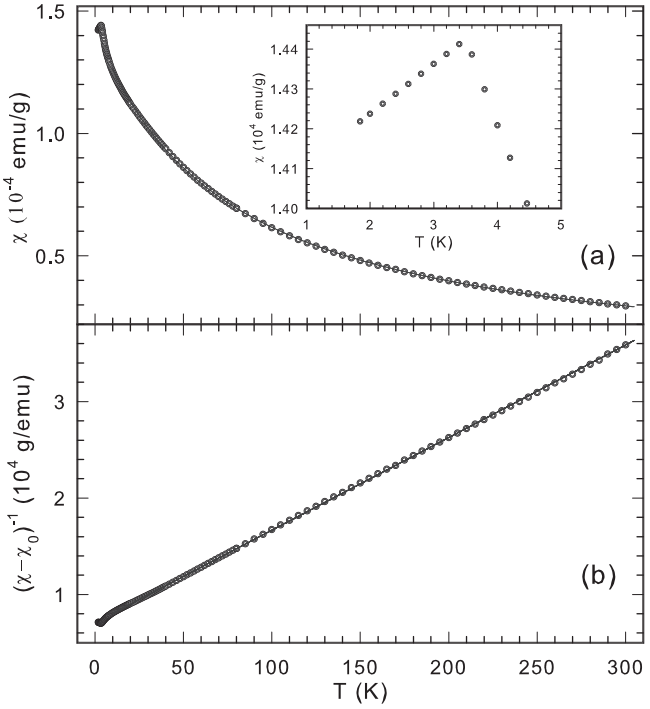

Fig. 2. (a) The temperature dependence of the magnetic susceptibility of the 1/1 approximant $Ag_{42}In_{42}Gd_{16}$, measured in an external magnetic field of 50 Oe. The solid line is the fit to Eq. (2) in the temperature range 20–300 K, as explained in the text. The inset shows the magnetic susceptibility data in the low-temperature range. (b) The inverse magnetic susceptibility corrected for the contribution χ_0, $(\chi - \chi_0)^{-1}$ versus temperature T of the of the 1/1 approximant $Ag_{42}In_{42}Gd_{16}$. The solid line is the fit to Eq. (2).

The temperature-independent magnetic susceptibility χ_0 consists of contributions from the Pauli susceptibility of conduction electrons and from the diamagnetic susceptibility of core electrons, $\chi_0 = \chi_P + \chi_d$. The latter is usually estimated as a weighted mean of the susceptibilities of the constituents of the alloy [20], and is thus $\chi_d = -1.33 \times 10^{-4}$ emu/(mol Gd) for the 1/1 approximant $Ag_{42}In_{42}Gd_{16}$. The value of χ_P is therefore $1.38(40) \times 10^{-3}$ emu/(mol Gd). The derived value of χ_P is comparable to that found in other single-crystalline Gd-containing alloys [21].

The theoretical value of $\mu_{eff}^{th} = g\mu_B\sqrt{J(J+1)}$ for a free Gd^{3+} ion (electronic configuration $^8S_{7/2}$), is 7.94 μ_B [22]. From the fact that the experimental value $\mu_{eff} = 7.86(23)$ μ_B is close to the theoretical value of 7.94 μ_B it is concluded that the magnetic moment is localized on the Gd^{3+} ions and that, as expected, Ag and In atoms carry no magnetic moment. The negative value of Θ_p indicates that the interaction between the Gd^{3+} spins is predominantly antiferromagnetic.

The nature of the magnetic transition at 3.4 K was determined by measuring the temperature dependence of the ZFC and FC magnetic susceptibility between 2 and 10 K in an applied magnetic field of 50 Oe (Fig. 3). There is a clear bifurcation between the ZFC and FC data at the freezing temperature $T_f = 3.4(1)$ K. Both ZFC and FC data are essentially identical above T_f. Such a behavior of the ZFC and FC susceptibility data is characteristic of a spin glass [23].

Both randomness and frustration are required for the occurrence of spin-glass behavior [23,24]. An empirical measure of frustration is the frustration parameter f, that is defined as $f = -\Theta_p/T_f$ [25]. Compounds with $f > 10$ are categorized as strongly geometrically frustrated compounds [25]. The value of f for the 1/1 approximant $Ag_{42}In_{42}Gd_{16}$ is 21.7(8). It should be compared with the value $f = 8.7$ for the *i* QC $Ag_{50}In_{36}Gd_{14}$ [7]. The 1/1 approximant

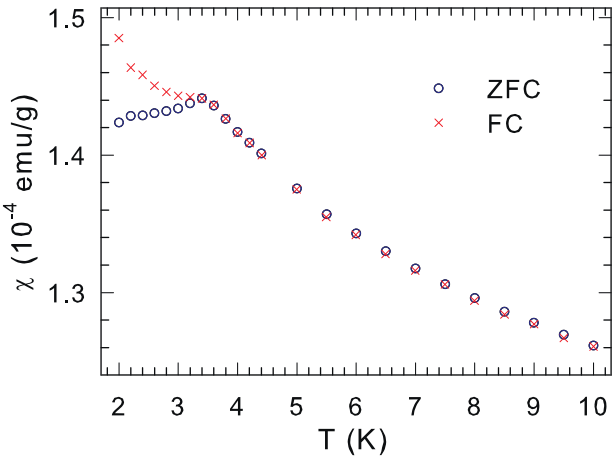

Fig. 3. The temperature dependence of the ZFC and FC magnetic susceptibility of the 1/1 approximant $Ag_{42}In_{42}Gd_{16}$, measured in an external magnetic field of 50 Oe.

$Ag_{50}In_{36}Gd_{14}$ thus belongs to a category of strongly geometrically frustrated magnets.

3.2.2. Ac magnetic susceptibiity

The temperature dependence of the in-phase component χ' of the ac magnetic susceptibility of the 1/1 approximant $Ag_{42}In_{42}Gd_{16}$ for different frequencies between 300 Hz and 10 kHz is shown in Fig. 4. The position of the maximum in $\chi'(T)$ can be used to define the freezing temperature T_f. The temperature of the maximum in $\chi'(T)$ and its error were extracted from a spline fit of the $\chi'(T)$ data (inset in Fig. 4). The $\chi'(T)$ curves show maxima whose amplitudes and positions depend on the frequency f of the applied ac magnetic field. With increasing frequency, the peak positions are shifted slightly to higher temperatures and the peak intensity of $\chi'(T)$ decreases. These features are typical for canonical spin glasses [23]. The frequency dependence of T_f is shown in Fig. 5. A quantitative measure of the change of the freezing temperature with frequency in spin glasses is represented by the relative change in T_f per decade change in f defined as [23]

$$K = \frac{\Delta T_f}{T_f \Delta \log f}. \quad (3)$$

From a linear fit of the data in Fig. 5, and using the average value of $T_f = 3.60$ K for the range of frequencies used, the value of $K = 0.0056(15)$ was obtained. This value is comparable to those

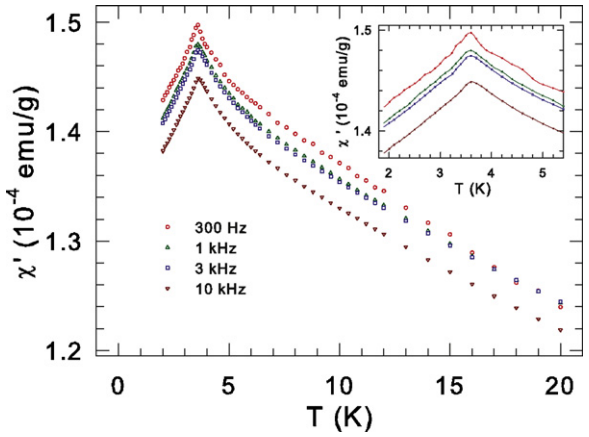

Fig. 4. The temperature dependence of the in-phase magnetic susceptibility χ' measured for different applied frequencies from 300 Hz to 10 kHz for the 1/1 approximant $Ag_{42}In_{42}Gd_{16}$. The inset shows a magnification of the low-temperature region. The solid curves are spline fits through the data.

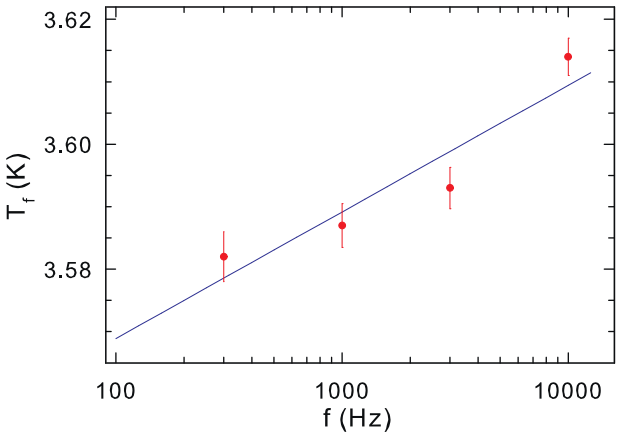

Fig. 5. The frequency dependence of the freezing temperature T_f for the 1/1 approximant $Ag_{42}In_{42}Gd_{16}$. The solid line is the best linear fit to the T_f data.

found for such canonical spin glasses as $Cu_{1-x}Mn_x$ ($K = 0.005$), $Au_{1-x}Mn_x$ ($K = 0.0045$), and $Ag_{1-x}Mn_x$ ($K = 0.006$) [23], and is two times smaller than the value of K for the i QC $Ag_{50}In_{36}Gd_{14}$ [7]. One notes that the value of K reported for another i QC $Tb_9Mg_{34}Zn_{57}$ is 0.049 [26].

The spin-glass freezing process can be interpreted in two different ways. In the first interpretation the existence of spin clusters is assumed and, in this case, the freezing is a nonequilibrium phenomenon [27]. In the second interpretation one presupposes the existence of a true equilibrium phase transition at a finite temperature [28]. For magnetically interacting clusters, the frequency dependence of T_f is described by the phenomenological Vogel–Fulcher law [23,27]

$$f = f_0 \exp\left[-\frac{E_a}{k_B}(T_f - T_0)\right], \quad (4)$$

where f_0 is a characteristic frequency, E_a is the activation energy, and T_0 is the Vogel–Fulcher temperature which is a measure of the interaction strengths between clusters in the spin glass [29]. Eq. (4) implies a linear dependence of $1/(T_f - T_0)$ with $\log(f)$. The best fit of the $T_f(f)$ data to Eq. (4) (Fig. 6), assuming $f_0 = 1 \times 10^{13}$ Hz as typically observed for other spin glasses [27], gives $E_a/k_B = 6.42(85)$ K and $T_0 = 3.30(1)$ K. For this fit, a coefficient of determination [30] $r^2 = 0.9716$. Similarly to what was observed for other spin glasses [27], one finds that $T_0 < E_a/k_B$.

In the second interpretation of the spin freezing phenomenon, it is assumed that the characteristic relaxation time $\tau = 1/f$ of magnetic moments shows a critical slowing down when approaching

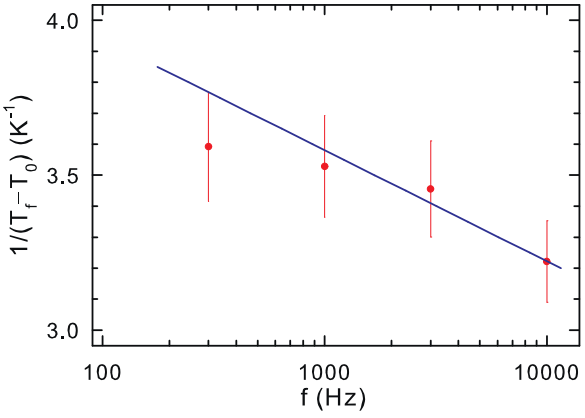

Fig. 6. The frequency dependence of the freezing temperature T_f for the 1/1 approximant $Ag_{42}In_{42}Gd_{16}$. The solid line is the best fit to Eq. (4).

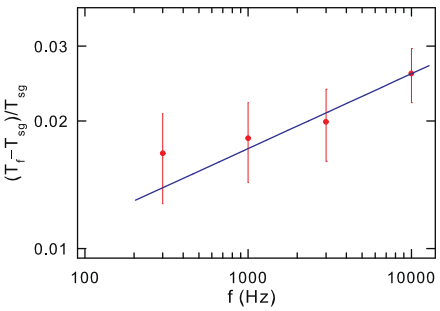

Fig. 7. The frequency dependence of the freezing temperature T_f for the 1/1 approximant $Ag_{42}In_{42}Gd_{16}$. The solid line is the best fit to Eq. (5).

T_f from above, characterized by a power law $\tau \propto \xi^z$, where ξ is the correlation length and z is the dynamic scaling exponent [31]. The correlation length ξ itself is related to the reduced temperature $t = (T_f - T_{sg})/T_{sg}$ as $\xi \propto t^{-\nu}$, where T_{sg} is the phase-transition temperature and ν is the critical correlation-length exponent [31]. Thus, the temperature dependence of f follows the power-law divergence [23,31]

$$f = f_0\left(\frac{T_f - T_{sg}}{T_{sg}}\right)^{z\nu}, \quad T_f > T_{sg}, \quad (5)$$

where f_0 is the microscopic relaxation time. The best fit of the $T_f(f)$ data in Fig. 7 to Eq. (5), assuming $f_0 = 1 \times 10^{13}$ Hz as typically observed for other spin glasses [27], yields $T_{sg} = 3.52(1)$ K and $z\nu = 5.65(21)$. For this fit, $r^2 = 0.9854$. The derived value of $z\nu$ falls in the range 4–12 of $z\nu$ values found for many different spin glasses [23,32].

The larger value of r^2 corresponding to the fit of the $T_f(f)$ data to Eq. (5) than to Eq. (4) indicates that the spin freezing in the 1/1 approximant $Ag_{42}In_{42}Gd_{16}$ is a phase transition rather than a nonequilibrium phenomenon.

3.3. Mössbauer spectroscopy

The ^{155}Gd Mössbauer spectrum of the 1/1 approximant $Ag_{42}In_{42}Gd_{16}$ measured at 4.6 K, i.e., in the paramagnetic region above T_f, is shown in Fig. 8. The site at which the Gd^{3+} ions are located has the point symmetry m [11], which implies a non-zero EFG at the Gd^{3+} site, and hence a non-zero electric quadrupole hyperfine interaction. The Mössbauer spectrum in Fig. 8 indeed shows the presence of a substantial electric quadrupole hyperfine

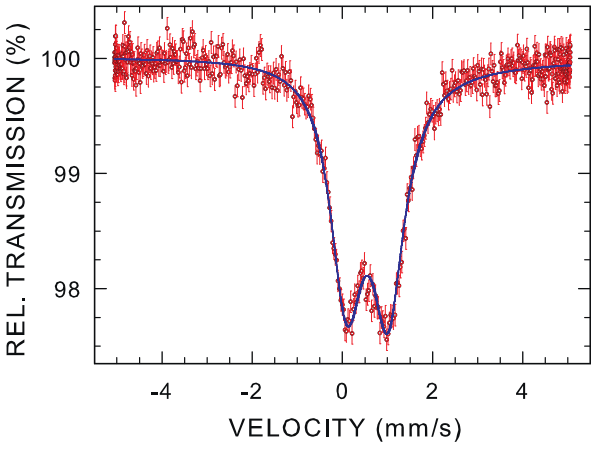

Fig. 8. The ^{155}Gd Mössbauer spectrum of the 1/1 approximant $Ag_{42}In_{42}Gd_{16}$ at 4.6 K fitted (solid line) with an electric quadrupole hyperfine interaction. The zero-velocity origin is relative to the source.

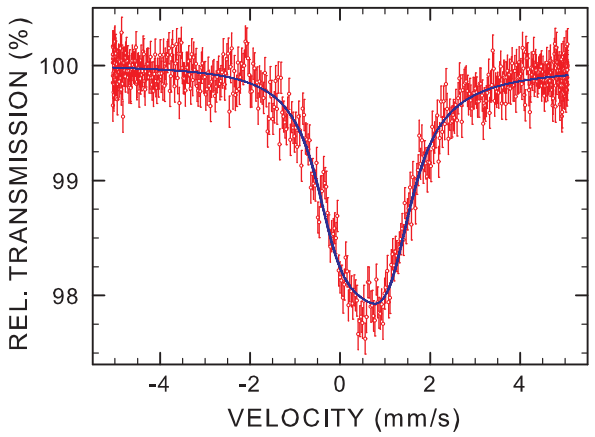

Fig. 9. The ^{155}Gd Mössbauer spectrum of the 1/1 approximant $Ag_{42}In_{42}Gd_{16}$ at 1.5 K fitted (solid line) with a combined magnetic dipole and electric quadrupole hyperfine interactions. The zero-velocity origin is relative to the source.

interaction and the absence of the magnetic dipole hyperfine interaction. The absence of the magnetic dipole hyperfine interaction in the Mössbauer spectrum in Fig. 8 proves that at 4.6 K the Gd spins are not in a frozen state. For ^{155}Gd nuclei, the quadrupole moment of the excited nuclear state $Q_{ex} = 0.12$ b [16], is significantly smaller than that of the ground nuclear state $Q_g = 1.30$ b [33]. Consequently, the quadrupole splitting of the excited nuclear state, which is sensitive to the sign of V_{zz} and the magnitude of η, is smaller than the natural linewidth $\Gamma_{nat} = 0.250$ mm/s mm/s. As a result, only the absolute value of the effective quadrupole splitting parameter $\Delta_g^{eff} = eQ_g|V_{zz}|\sqrt{1+\eta^2/3}$ can be derived from a Mössbauer spectrum of a sample in the paramagnetic state [34]. The following parameters were derived from the fit ($\chi^2 = 1.14$) of the Mössbauer spectrum in Fig. 8: the isomer shift (relative to the ^{155}Eu(SmPd$_3$) source) $\delta = 0.542(5)$ mm/s, $\Delta_g^{eff} = 1.919(19)$ mm/s, $f_a = 10.4(1)$%, and $\Gamma_a = 0.494(15)$ mm/s. The value of δ confirms the trivalent state of Gd in the 1/1 approximant $Ag_{42}In_{42}Gd_{16}$ [34]. The value of Δ_g^{eff} is close to that for the *i* QC $Ag_{50}In_{36}Gd_{14}$ [7], which is indicative of a strong similarity of the local atomic structure around the Gd atoms in the 1/1 approximant $Ag_{42}In_{42}Gd_{16}$ and the *i* QC $Ag_{50}In_{36}Gd_{14}$.

For the lattice vibrations treated in terms of the Debye approximation, the absorber Debye–Waller factor f_a is expressed [15] by the Debye temperature, Θ_D, as

$$f_a(T) = \exp\left\{-\frac{3}{4}\frac{E_\gamma^2}{Mc^2 k_B \Theta_D}\left[1 + 4\left(\frac{T}{\Theta_D}\right)^2 \int_0^{\Theta_D/T} \frac{x\,dx}{e^x - 1}\right]\right\}, \quad (6)$$

where E_γ is the energy of the Mössbauer transition, M is the mass of the Mössbauer nucleus, and c is the speed of light. The value of $f_a = 10.4(1)$% derived from the fit of the Mössbauer spectrum in Fig. 8 gives via Eq. (6) $\Theta_D = 200(1)$ K, which is the same as Θ_D of the *i* QC $Ag_{50}In_{36}Gd_{14}$ [7]. This means that the phonon dynamics in these two alloys is very similar. The low value of Θ_D of the 1/1 approximant $Ag_{42}In_{42}Gd_{16}$ compares well with the value of 145.2 K for the 1/1 approximant $YbCd_6$ derived from the specific heat data [35].

Fig. 9 shows the ^{155}Gd Mössbauer spectrum of the 1/1 approximant $Ag_{42}In_{42}Gd_{16}$ at 1.5 K, i.e., below T_f. This spectrum clearly exhibits the presence of a combined magnetic dipole and electric quadrupole hyperfine interactions. The presence of the magnetic dipole hyperfine interaction in the Mössbauer spectrum in Fig. 9 proves that the Gd spins are frozen at 1.5 K. The Mössbauer spectrum in Fig. 9 was fitted by fixing the value of Γ_a to 0.494 mm/s obtained from the fit of the 4.6 K Mössbauer spectrum, and the value of θ to 0.0°. The following parameters were derived from the fit ($\chi^2 = 1.01$) of the Mössbauer spectrum in Fig. 9: $\delta = 0.546(12)$ mm/s, $H_{hf} = 96.7(12.1)$ kOe, the quadrupole splitting constant $eQ_gV_{zz} = 1.937(25)$ mm/s ($V_{zz} = 4.30(8) \times 10^{21}$ V/m^2), $\eta = 0.1(2)$, and $f_a = 10.4(2)$%. A substantial value of H_{hf} indicates a considerable magnetic moment of Gd atoms.

4. Summary

A new 1/1 approximant $Ag_{42}In_{42}Gd_{16}$ to an icosahedral quasicrystal Ag–In–Gd has been studied with X-ray diffraction, dc and ac magnetic susceptibility, and ^{155}Gd Mössbauer spectroscopy. It is shown that this compound develops no long-range magnetic order, but is a spin glass with freezing temperature $T_f = 3.6(1)$ K. The frequency dependence of T_f can be described by the Vogel–Fulcher law and the power-law divergence. It is argued that the spin freezing process is not a nonequilibrium phenomenon but tather a true equilibrium phase transition. The ^{155}Gd Mössbauer spectra of the 1/1 approximant $Ag_{42}In_{42}Gd_{16}$ confirm that the Gd spins are frozen at 1.5 K and are fluctuating at 4.6 K. The Debye temperature of the 1/1 approximant $Ag_{42}In_{42}Gd_{16}$ is 200(1) K.

Acknowledgments

This work was supported by the Natural Sciences and Engineering Research Council of Canada. Support from the Polish Ministry of Science and Higher Education and the Structural Funds of the European Commission, Project No. SPO WKP 1.4.3 is gratefully acknowledged.

References

[1] D. Shechtman, I. Blech, D. Gratias, J.W. Cahn, Phys. Rev. Lett. 53 (1984) 1951.
[2] Z.M. Stadnik (Ed.), Physical Properties of Quasicrystals, Springer-Verlag, Berlin, 1999;
J.-B. Suck, M. Schreiber, P. Häussler (Eds.), Quasicrystals, An Introductions to Structure, Physical Properties, and Applications, Springer-Verlag, Berlin, 2002;
T. Fujiwara, Y. Ishii, Quasicrystals, Elsevier, Amsterdam, 2008.
[3] A.P. Tsai, J.Q. Guo, E. Abe, E. Takakura, T.J. Sato, Nature 408 (2000) 537;
J.Q. Guo, E. Abe, A.P. Tsai, Phys. Rev. B 62 (2000) R14605.
[4] J.Q. Guo, A.P. Tsai, Philos. Mag. Lett. 82 (2000) 349.
[5] S. Iwano, H. Nishimoto, R. Tamura, S. Takeuchi, Philos. Mag. 86 (2006) 435.
[6] Y.K. Kuo, K.M. Sivakumar, H.H. Lai, C.N. Ku, S.T. Lin, A.B. Kaiser, Phys. Rev. B 72 (2005) 054202.
[7] Z.M. Stadnik, K. Al-Qadi, P. Wang, J. Phys.: Condens. Matter 19 (2007) 326208.
[8] V. Elser, C.L. Henley, Phys. Rev. Lett. 55 (1985) 2883.
[9] A.I. Goldman, K.F. Kelton, Rev. Mod. Phys. 65 (1993) 213.
[10] H. Takakura, J.Q. Guo, A.P. Tsai, Philos. Mag. Lett. 81 (2002) 411.
[11] C.P. Gómez, S. Lidin, Phys. Rev. B 68 (2000) 024203.
[12] J.F. Ruan, K.H. Kuo, J.Q. Guo, A.P. Tsai, J. Alloys Compd. 370 (2004) L23.
[13] D.L. Bish, S.J. Chipera, Powder Diffract. 4 (1989) 137.
[14] B.F. Otterloo, Z.M. Stadnik, A.E.M. Swolfs, Rev. Sci. Instrum. 54 (1983) 1575.
[15] N.N. Greenwood, T.C. Gibb, Mössbauer Spectroscopy, Chapman and Hall, London, 1971;
P. Gütlich, R. Link, A. Trautwein, Mössbauer Spectroscopy and Transition Metal Chemistry, Springer, Berlin, 1978.
[16] H. Armon, E.R. Bauminger, S. Ofer, Phys. Lett. B 43 (1973) 380.
[17] Z.M. Stadnik, J. Żukrowski, unpublished.
[18] S. Margulies, J.R. Ehrman, Nucl. Instrum. Methods 12 (1961) 131;
G.K. Shenoy, J.M. Friedt, H. Maletta, S.L. Ruby, in: I.J. Gruverman, C.W. Seidel, D.K. Dieterly (Eds.), Mössbauer Effect Methodology, vol. 10, Plenum, New York, 1974, p. 277.
[19] R.A. Young, The Rietveld Method, Oxford University Press, Oxford, 1993.
[20] P.W. Selwood, Magnetochemistry, Interscience Publishers, New York, 1956.
[21] M.A. Avila, S.L. Bud'ko, P.C. Canfield, J. Magn. Magn. Mater. 270 (2004) 51;
A.S. Sefat, B. Li, S.L. Bud'ko, P.C. Canfield, Phys. Rev. B 76 (2007) 174419.
[22] N.W. Ashcroft, N.D. Mermin, Solid State Physics, Saunders, Philadelphia, 1976.
[23] J.A. Mydosh, Spin Glasses: An Experimental Introduction, Taylor & Francis, London, 1993.
[24] G. Toulouse, Commun. Phys. 2 (1977) 116;
K. Binder, A.P. Young, Rev. Mod. Phys. 58 (1986) 801.
[25] A.P. Ramirez, in: K.H.J. Buschow (Ed.), Handbook of Magnetic Materials, vol. 13, Elsevier, Amsterdam, 2001, p. 423.
[26] I.R. Fisher, K.O. Cheon, A.F. Panchula, P.C. Canfield, M. Chernikov, H.R. Ott, K. Dennis, Phys. Rev. B 59 (1999) 308.
[27] J.L. Tholence, Solid State Commun. 35 (1980) 113.
[28] S.F. Edwards, P.W. Anderson, J. Phys. F 5 (1975) 965.

[29] S. Shtrikman, E.P. Wohlfarth, Phys. Lett. A 85 (1981) 467.
[30] A. Senyshyn, D.M. Trots, J.M. Engel, L. Vasylechko, H. Ehrenberg, T. Hansen, M. Berkowski, H. Fuess, J. Phys.: Condens. Matter 21 (2009) 145405.
[31] P.C. Hohenberg, B.I. Halperin, Rev. Mod. Phys. 49 (1977) 435.
[32] J. Souletie, J.L. Tholence, Phys. Rev. B 32 (1985) 516.
[33] Y. Tanaka, D.B. Laubacher, R.M. Steffen, E.B. Shera, H.D. Wohlfahrt, M.V. Hoehn, Phys. Lett. B 108 (1982) 8.
[34] G. Czjzek, in: G.J. Long, F. Grandjean (Eds.), Mössbauer Spectroscopy Applied to Magnetism and Materials Science, vol. 1, Plenum, New York, 1993, p. 373.
[35] S.K. Dhar, A. Palenzona, P. Manfrinetti, S.M. Pattalwar, J. Phys.: Condens. Matter 13 (2002) 517.